Uncharged S4 Residues and Cooperativity in Voltage-dependent Potassium Channel Activation

Catherine J. Smith-Maxwell,*‡ Jennifer L. Ledwell,*‡ and Richard W. Aldrich*‡

From the *Department of Molecular and Cellular Physiology, and ‡Howard Hughes Medical Institute, Stanford University, Stanford, California 94305

ABSTRACT Substitution of the S4 of Shaw into Shaker alters cooperativity in channel activation by slowing a cooperative transition late in the activation pathway. To determine the amino acids responsible for the functional changes in Shaw S4, we created several mutants by substituting amino acids from Shaw S4 into Shaker. The S4 amino acid sequences of Shaker and Shaw S4 differ at 11 positions. Simultaneous substitution of just three non-charged residues from Shaw S4 into Shaker (V369I, I372L, S376T; ILT) reproduces the kinetic and voltage-dependent properties of Shaw S4 channel activation. These substitutions cause very small changes in the structural and chemical properties of the amino acid side chains. In contrast, substituting the positively charged basic residues in the S4 of Shaker with neutral or negative residues from the S4 of Shaw S4 does not reproduce the shallow voltage dependence or other properties of Shaw S4 opening. Macroscopic ionic currents for ILT could be fit by modifying a single set of transitions in a model for Shaker channel gating (Zagotta, W.N., T. Hoshi, and R.W. Aldrich. 1994. *J. Gen. Physiol.* 103:321–362). Changing the rate and voltage dependence of a final cooperative step in activation successfully reproduces the kinetic, steady state, and voltage-dependent properties of ILT ionic currents. Consistent with the model, ILT gating currents activate at negative voltages where the channel does not open and, at more positive voltages, they precede the ionic currents, confirming the existence of voltage-dependent transitions between closed states in the activation pathway. Of the three substitutions in ILT, the I372L substitution is primarily responsible for the changes in cooperativity and voltage dependence. These results suggest that noncharged residues in the S4 play a crucial role in Shaker potassium channel gating and that small steric changes in these residues can lead to large changes in cooperativity within the channel protein.

KEY WORDS: Shaker • gating • ion channel • patch clamp

INTRODUCTION

The S4 segment of voltage-gated ion channels participates in sensing the membrane voltage and in the conformational changes leading to channel opening (Yang and Horn, 1995; Aggarwal and MacKinnon, 1996; Mannuzzu et al., 1996; Larsson et al., 1996; Seoh et al., 1996; Yusaf et al., 1996; Yang et al., 1996). In the preceding paper, we examined the properties of Shaker channels with S4 segments substituted from other related channels (Smith-Maxwell et al., 1998). We found that the slopes and positions of the conductance–voltage curves in the several S4 chimeras do not correlate with the nominal charge content of the S4. Instead, we found that cooperative interactions between subunits play a major role in determining the voltage dependence of channel activation. A closer examination of the Shaw S4 chimera and of heterodimers with Shaker and Shaw S4 subunits revealed that a highly coopera-

tive step in the activation pathway is rate limiting. These findings are consistent with a role for the S4 in channel activation that involves not only sensing voltage, but also somehow mediating cooperative interactions between channel subunits.

In this paper, we investigate the molecular basis for the changes in activation gating observed in the Shaw S4 substitution. We constructed mutants in Shaker with combinations of amino acids substituted from Shaw S4 to determine the amino acids in Shaw S4 responsible for the altered gating behavior. We use the information from changes in the position and slope of the conductance–voltage curve and also changes in kinetics and in sigmoidicity of the activation time course to interpret the effects introduced by amino acid substitutions. Changes in sigmoidicity are diagnostic of changes in the kinetic mechanism of activation, providing information about changes in the relative contributions of the many conformational changes in the activation pathway (Zagotta et al., 1994a; Smith-Maxwell et al., 1998). We interpret the changes in gating of mutant channels in terms of a kinetic scheme developed previously for Shaker that closely fits macroscopic ionic, single channel, and gating currents (Zagotta et al., 1994a). We identify a set of transitions that are altered by the

Address correspondence to Dr. Richard W. Aldrich, Dept. of Molecular and Cellular Physiology, Stanford University, Beckman Center, B171, Stanford, CA 94305-5426. Fax: 650-725-4463; E-mail: raldrich @leland.stanford.edu

substitutions and show that a single, conservative amino acid substitution is primarily responsible for the change in cooperativity. Our study shows that steric interactions of noncharged residues are likely to play an important role in the activation process and mediate cooperative interactions between subunits. Preliminary reports of these findings have been presented in abstract form (Smith-Maxwell et al., 1993, 1994; Ledwell et al., 1997).

MATERIALS AND METHODS

Molecular Biology

All constructs in the Shaker background were made in a form of Shaker mutant, ShBΔ6-46, in which fast N-type inactivation was removed and silent restriction enzyme sites were added (Smith-Maxwell et al., 1998). Construction of the Shaw S4 chimera was described in the preceding paper (Smith-Maxwell et al., 1998). All other mutations made in the Shaker background were generated by PCR-mediated cassette mutagenesis. DNA fragments with mutations generated by PCR were inserted between naturally occurring unique restriction enzyme sites in the channel construct, StyI and NsiI. All mutations were verified by dideoxy termination sequencing (Sanger et al., 1977). Single amino acid substitutions are identified by their residue number. Identification of the substitutions in each multiple mutant is as follows: ESS-R362E, R365S, K380S; EFFSII-R362E, V363F, I364F, R365S, L366I, V367I; FIIT-I364F, L366I, V369I, S376T; ILT-V369I, I372L, S376T; IL-V369I, I372L; LT-I372L, S376T; IT-V369I, S376T (Fig. 1). We were unable to detect currents from two other multiple point mutants we constructed: FIML-V363F, L366I, F370M, I372L and IMLTS-V367I, F370M, I372L, S376T, K380S. Numbering of amino acids is from Schwarz et al. (1988) for the ShB1 potassium channel.

A highly expressing ILT construct was made by substituting the mutant ILT sequence into a high expression Shaker (W434F) vector obtained from Ligia Toro (Perozo et al., 1993). DNA from the original ILT mutant was cut between the BsiWI and SpeI restriction enzyme sites, generating a fragment that includes the ILT S4 and the Shaker wild-type tryptophan residue at position 434. This piece of DNA was substituted into the W434F Shaker construct, creating a conducting form of ILT that expressed at high levels.

The VIS/Shaw triple point mutant, constructed in the Shaw background, was made by annealing sense and antisense oligonucleotides spanning two naturally occurring restriction enzyme sites in the Shaw sequence, ClaI and StyI. Substitutions for the point mutations were made in Shaw at the following sites, using numbering from Butler et al. (1989): VIS/Shaw-I302V, L305I, T309S (see Fig. 1).

Expression System and Electrophysiology

Xenopus oocytes were used for functional expression of mutant DNA channel constructs, as described in the previous paper (Smith-Maxwell et al., 1998). For Shaker and all mutants in the Shaker background, cRNA was made from KpnI-linearized DNA with T7 RNA polymerase. For Shaw and VIS/Shaw, cRNA was made from SacI- or SalI-linearized DNA with T3 RNA polymerase.

Macroscopic ionic currents were measured from inside-out membrane patches as previously described (Smith-Maxwell et al., 1998; Hamill et al., 1981), using Mg^{++}-free intracellular solutions for constructs requiring large positive voltage steps to activate. Ionic currents were digitized at 5–50 kHz and low pass filtered with an eight-pole Bessel filter at 2–9 kHz, depending on the channel kinetics. Details are stated in the figure legends.
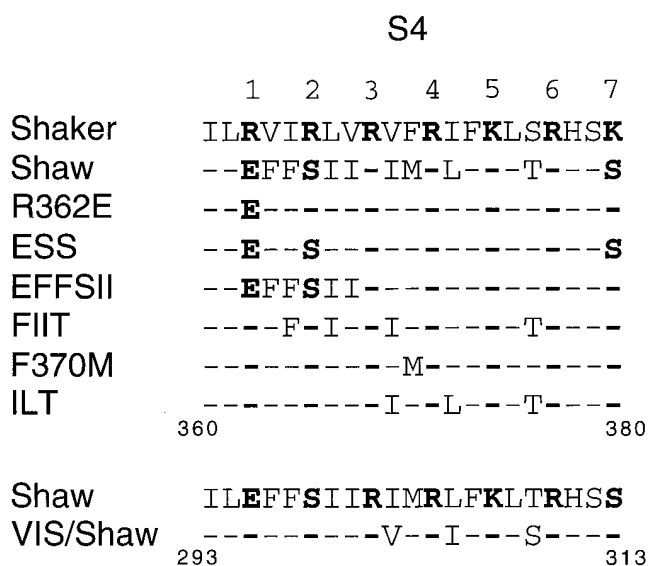

FIGURE 1. S4 Sequences for wild-type Shaker, Shaw, and mutant channels. The standard single letter code is used to designate amino acids at each position. Basic residues are identified by number above the sequences from the amino terminal to the carboxy terminal end of the S4. Letters or dashes located at positions containing basic residues in Shaker are in bold for all sequences. (*top*) Dl a termino-nus and are taken from Tempel et al. (1987). (*bottom*) Dashes indicate amino acids identical to Shaw. The numbers below identify the amino acids in the sequence based on the numbering scheme of Butler et al. (1989).

Gating currents were measured using a high performance cut-open oocyte voltage clamp (CA-1; Dagan Corp., Minneapolis, MN) (Taglialatela et al., 1992). The oocytes were permeabilized with 0.3% saponin. Agar bridges with platinum iridium wire were filled with 1 M NaMES (sodium methanesulfonic acid). Microelectrodes were filled with 3 M KCl and had tip resistances of <1 MΩ. The following solutions were used for measurement of gating currents. The internal solution included (mM): 110 KOH, 2 $MgCl_2$, 1 $CaCl_2$, 10 EGTA, 5 HEPES, pH 7.1 with MES. The external solution included (mM): 110 NaOH, 2 KOH, 2 $MgCl_2$, 5 HEPES, pH 7.2 with MES. Nonlinear capacitive currents of comparable amplitude and decay rate were never observed in uninjected oocytes.

All experiments were carried out at 20 ± 0.2°C.

Data Analysis

The voltage dependence of channel opening was estimated from the normalized conductance calculated two different ways as outlined in Smith-Maxwell et al. (1998). Normalized chord conductance was used for ShBΔ6-46, R362E, ESS, EFFSII, F370M, V369I, and S376T. Normalized conductance was calculated from isochronal measurements of tail currents after the peak current for FIIT, ILT, Shaw S4, IL, LT, IT, I372L, VIS/Shaw, and Shaw. Conductance–voltage curves were fit with first or fourth power Boltzmann functions as follows:

$$\frac{G}{G_{max}} = \left(\frac{1}{1 + e^{-zF(V - V_{1/2})/RT}} \right)^n$$

with n equal to 1 or 4. For a first power Boltzmann function, $V_{1/2}$ is the voltage at which channel opening is half maximal. For a fourth power Boltzmann, $V_{1/2}$ approximates the voltage at which each subunit is activated half maximally. The slope factor is equal to RT/zF.

Activation kinetics were quantified by fitting the activation time course of macroscopic ionic currents with the following exponential function: $I(t) = A[1 - e^{(-t + d)/\tau}]$.

$I(t)$ is the current at time t, A is the scale factor for the fit, τ is the time constant, and d is the delay or amount of time required to shift the single exponential curve along the time axis to obtain an adequate fit of the activation time course. The time course of most currents could be fit with this function from a beginning current level of 2–5% up to the maximum current level. Large sigmoidal delays such as those seen with Shaker cause currents to deviate significantly from single exponential behavior early in activation, making it necessary for single exponential fits to begin at 20–50% of the maximum current. Time constants for deactivation were obtained from fits of a single exponential to tail currents measured at negative membrane potentials. Tail currents were generally well fit by a single exponential function.

Analysis of the sigmoidicity in activation kinetics was carried out as described previously (Zagotta et al., 1994a, 1994b; Smith-Maxwell et al., 1998). Briefly, currents are first scaled so that all traces reach the same maximum value. Then the scaling of the currents along the time axis is changed so that the slope at the half maximal current level is the same for all traces. This method of analysis allows comparison of the delay in the activation kinetics relative to the overall time course of channel opening. When channel opening follows a single exponential time course with no delay, the relative time to half maximum current (thmx) is defined as equal to one. Relative thmx values greater than one indicate the presence of a delay in channel opening (see Fig. 4 C).

Simulations of macroscopic currents were carried out as described previously (Zagotta et al., 1994b; Smith-Maxwell et al., 1998). Rate constants in the 15-state model used here to describe ILT and I372L macroscopic currents are taken from a model described previously for the Shaker potassium channel (see Fig. 7 and Table I in Zagotta et al., 1994a). Only transitions between the last closed and open states are altered to simulate mutant macroscopic currents.

R E S U L T S

Substitution of S4 segments in Shaker can decrease the apparent voltage dependence of channel opening by changing cooperative interactions between the subunits, separate from changes due to decreased gating charge (Smith-Maxwell et al., 1998). The most pronounced changes in channel activation were introduced by substitution with the S4 of Shaw. Shaw S4 activation is shifted $\sim +120$ mV to more positive voltages and activates with 2.7-fold less apparent voltage dependence than Shaker (Fig. 2, Table I). The rate of Shaw S4 opening is much slower than the rate of Shaker opening and is shifted along the voltage axis in the same direction as the probability of channel opening. Shaw S4 activation kinetics follow a single exponential time course over a wide voltage range, unlike Shaker, which activates at most voltages with a large sigmoidal delay. All of these changes in macroscopic currents can be accounted for qualitatively by making a single coopera-

tive transition in the activation pathway rate limiting (Smith-Maxwell et al., 1998).

In this paper, we determine which amino acids in the S4 sequence of Shaw S4 are responsible for the functional differences between Shaw S4 and Shaker. As shown in Fig. 1, the S4 sequences of Shaw and Shaker differ in 11 of 21 positions. We generated several mutant Shaker potassium channels with single or multiple point mutations, substituting residues from the S4 of Shaw into Shaker in various combinations (Fig. 1). Representative macroscopic current traces and normalized conductance–voltage curves from several patches for each mutant are illustrated in Fig. 2. Results obtained from analysis of the conductance–voltage curves for each channel species are summarized in Table I.

While the total gating charge per channel determines the slope of the conductance–voltage relation at very low open probabilities (Almers, 1978; Schoppa et al., 1992; Zagotta et al., 1994a, 1994b; Sigg and Bezanilla, 1997), it does not reflect the contributions to channel gating from interactions between subunits (Sigworth, 1993; Zagotta et al., 1994a). Since we are interested in all effects of S4 substitutions on channel opening, we focused our attention on the slope of the conductance–voltage relation at moderate open probabilities where contributions from both charge and cooperativity are reflected in channel opening. We use "slope" as distinguished from "limiting slope" to refer to the steepness of the conductance–voltage relation in the range of moderate open probabilities.

Substitution of S4 Basic Residues

Extensive evidence in the literature supports the hypothesis that the S4 in voltage-gated cation channels is part of the voltage sensor and that S4 basic residues provide much of the gating charge (Yang and Horn, 1995; Aggarwal and MacKinnon, 1996; Seoh et al., 1996; Larsson et al., 1996; Mannuzzu et al., 1996; Yusaf et al., 1996; Yang et al., 1996). Because the basic residues play an important role in channel activation, we focused first on three amino acid differences between Shaker and Shaw S4 that occur at positions where Shaker has basic residues and Shaw S4 does not. Two of the substitutions exchange neutral serines for the basic residues at positions 2 and 7 in the S4 of Shaker and the other substitution exchanges, such as negatively charged glutamate for the positively charged arginine at position 1 (see Fig. 1). We studied several mutants in which one or more of these three basic residues were substituted, including R362E, ESS, and EFFSII (Fig. 2, Table I). The ESS mutant has substitutions at all three basic residues, which results in a decrease in nominal net charge of the S4 from +7 in Shaker to +3 in ESS. Such a large decrease in charge content of the S4 might be expected to alter profoundly the voltage de-
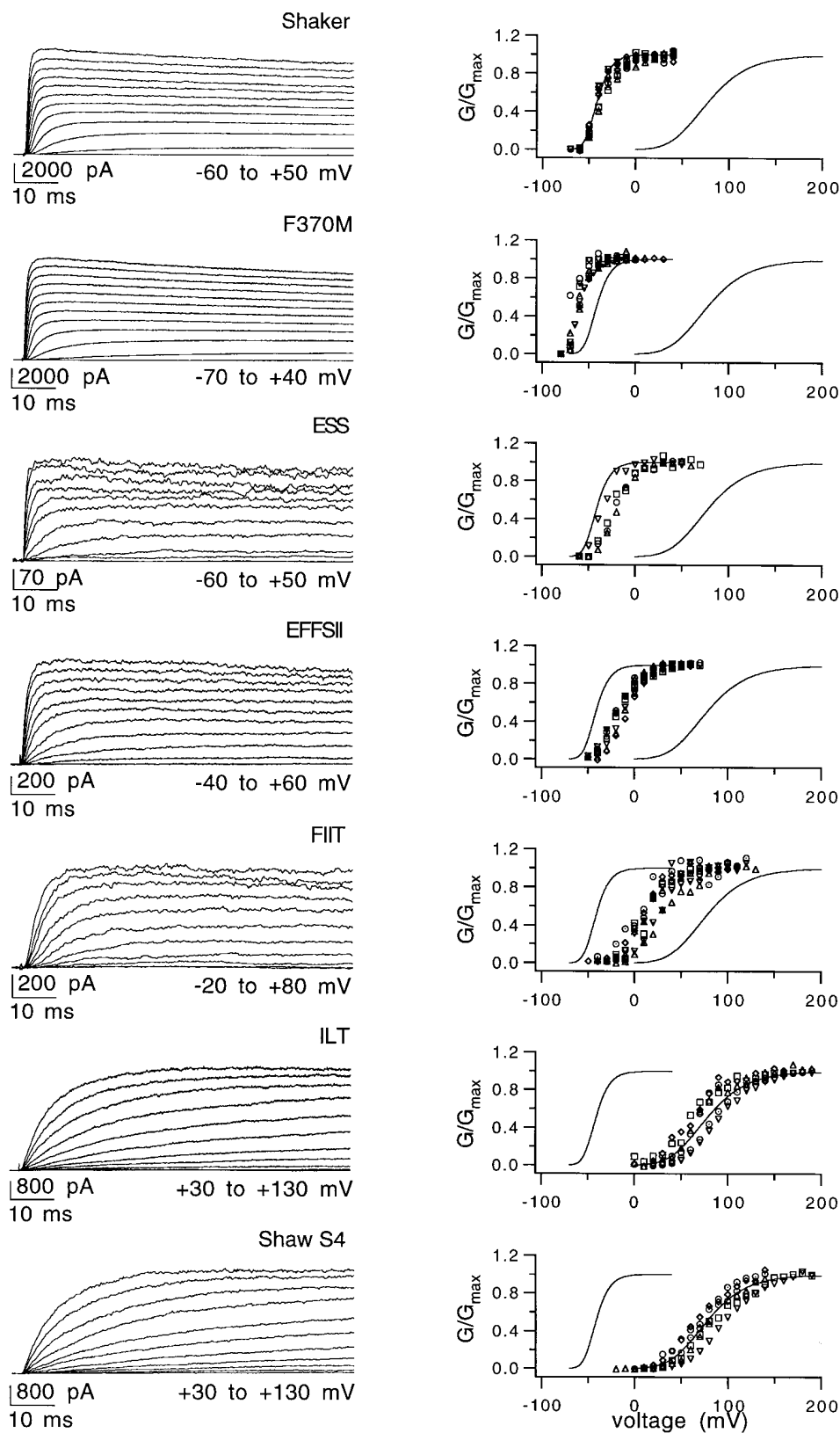
FIGURE 2. Macroscopic currents and conductance–voltage curves for channels with single and multiple point mutations in the S4 of Shaker. On the left are examples of currents from each channel construct recorded from inside-out patches in the voltage ranges indicated. All traces are incremented by 10 mV. On the right are conductance–voltage curves normalized to the maximum conductance at more positive voltages. Each symbol represents a separate experiment. The lines are fourth power Boltzmann functions, as outlined in MATERIALS AND METHODS, generated from the mean values in Table I for Shaker and Shaw S4 and are included to ease comparison between the mutants, Shaker, and Shaw S4 (see Smith-Maxwell et al., 1998). Currents from ILT and Shaw S4 were digitized at 5 kHz and filtered at 2 kHz. All other currents were digitized at 20 kHz and filtered at 2 kHz. The number of patches represented in each graph is as follows: eight for Shaker, eight for F370M, four for ESS, nine for EFFSII, eight for FIIT, six for ILT, and six for Shaw S4.

Boltzmann Relation Fits Comparing Mutants

Channel	Fourth power Boltzmann				First power Boltzmann				n
	$V_{1/2}$	SEM	Slope	SEM	$V_{1/2}$	SEM	Slope	SEM	
	mV		*mV*		*mV*		*mV*		
ShBΔ6-46	−56.9	±0.7	9.2	±1.0	−40.0	±1.2	6.8	±0.8	8
R362E	−49.4	±1.8	14.8	±0.6	−24.0	±1.2	11.1	±0.4	5
ESS	−46.3	±2.8	12.4	±0.7	−24.9	±3.5	9.2	±0.5	4
EFFSII	−41.1	±2.0	15.5	±0.5	−14.7	±1.7	11.4	±0.3	8
FIIT	−16.8	±2.8	18.1	±0.8	+14.2	±3.5	13.1	±0.6	8
F370M	−73.3	±1.2	6.2	±0.6	−62.1	±1.5	4.5	±0.5	8
ILT	+34.8	±5.1	22.3	±1.5	+72.3	±5.3	15.4	±1.6	6
V369I	−44.4	±1.5	12.5	±0.7	−22.2	±1.5	9.7	±0.6	9
I372L	−19.1	±2.6	19.8	±1.1	+14.5	±3.6	14.4	±0.8	4
S376T	−51.5	±4.6	16.8	±1.8	−22.0	±3.5	12.9	±1.5	5
IL	−25.2	±5.6	11.4	±3.9	−1.9	±2.3	8.6	±2.7	3
LT	+1.9	±2.4	18.9	±1.6	+34.4	±4.6	13.4	±1.1	4
IT	−20.0	±3.4	17.4	±1.8	+10.6	±2.8	13.0	±1.3	4
Shaw S4	+32.6	±4.9	26.8	±2.0	+77.6	±4.5	18.7	±1.4	7

Data from individual patches were fit with first and fourth power Boltzmann functions as outlined in MATERIALS AND METHODS. The values of $V_{1/2}$ and slope are means computed from the indicated number of patches, *n*.

pendence of channel gating. Surprisingly, changes in channel opening introduced by the ESS mutant are relatively modest compared with the changes introduced by the total S4 of Shaw. The voltage range of activation is shifted only +10 mV and the slope of the conductance–voltage curve is only slightly decreased. In fact, for all three of the mutants (R362E, ESS, EFFSII), the slope is roughly the same, regardless of whether one, two, or three basic residues are substituted. Thus, there is no correlation between the nominal charge content of the S4 and the position and slope of the conductance–voltage curve. All three mutant channels activate quickly, like Shaker but unlike Shaw S4.

These results show that the substituted basic residues in Shaw S4 are not responsible for the large changes observed in the voltage-dependent behavior of the macroscopic ionic currents. The results could be interpreted to mean that basic amino acids at positions 1, 2, and 7 of the S4, lying at either end of the S4 segment, contribute minimally to the activation process of Shaker potassium channels compared with the four remaining basic residues within the core of the segment. This does not seem to be the case, however, because experiments measuring the individual contribution to the gating charge of each of the S4 basic residues in Shaker suggest that basic residues at positions 1–5 contribute substantially to the gating charge (Aggarwal and MacKinnon, 1996; Seoh et al., 1996). An alternative interpretation is suggested by the results and conclusions in our preceding paper. The decrease in S4 charge in R362E, ESS, and EFFSII may be masked because the shape and

position of the conductance–voltage curve are dominated by cooperativity between subunits.

Substitution of S4 Nonbasic Residues

We studied several mutants with substitutions of nonbasic residues from Shaw S4 into Shaker. One mutant, EFFSII, in addition to substitution of the first two basic residues in the S4, includes four hydrophobic substitutions in the NH_2-terminal half of the S4. The changes in activation introduced by the substitutions in the EFFSII mutant are small compared with those introduced in the Shaw S4 chimera. This result suggests that the NH_2-terminal half of the S4 is not responsible for the major differences between the functional properties of Shaw S4 and Shaker.

There are five residues in the COOH-terminal half of the S4 that differ between Shaw S4 and Shaker. Several mutant channels were constructed with overlapping combinations of amino acid substitutions in this region. Among these mutants, only FIIT, F370M, and ILT expressed functional channels. The FIIT mutant opens with a steady state voltage dependence intermediate between Shaker and Shaw S4 (Table I), but it activates relatively rapidly and with a sigmoidal time course similar to Shaker.

The F370M mutant was generated by the substitution of methionine for a phenylalanine normally present in the middle of the Shaker S4. As shown in Fig. 2, activation kinetics are fast and sigmoidal, like Shaker. This is the only mutant we examined where the probability of channel opening is shifted to more negative voltages. All of the other mutations reported here, like most S4 mutations in the literature, shift the probability of channel opening to more positive voltages. However, a few S4 mutations that negatively shift activation have been reported (Lopez et al., 1991; Papazian et al., 1991; Liman et al., 1991; Logothetis et al., 1992, 1993). The F370M mutant also differs from most other S4 mutants in that C-type inactivation is dramatically affected. The channel inactivates much more rapidly than Shaker and recovers from inactivation very slowly (data not shown). Also, tail currents measured during channel closing are very slow compared with Shaker (data not shown).

Of the subsets of Shaw S4 amino acid replacements, only ILT had macroscopic ionic currents similar to Shaw S4 (Fig. 2, Table I). Activation kinetics of ILT are slow and single exponential over a wide range of voltages, like Shaw S4. The voltage range and slope of the conductance–voltage curve appear very similar to Shaw S4 as well. Since none of these three substitutions change the basic residues in the S4, the decrease in the slope of the conductance–voltage curve cannot be the result of decreasing the charge content of the S4. Our results are consistent with the idea that the S4 substitu-

tions, V369I, I372L, and S376T, are responsible for the change in cooperativity of the activation process seen in Shaw S4.

Substitutions of Subsets of ILT

Individual substitution of any one of the amino acids in the ILT mutant is not sufficient to cause Shaker to behave like ILT. Representative currents from the V369I, I372L, and S376T mutants along with normalized conductance–voltage curves from several patches are shown in Fig. 3. Boltzmann fits to the conductance–voltage curves are summarized in Table I. Considerable changes in the voltage range of activation and the slope of the conductance–voltage curve are seen with each of the three point mutants, but all activate with relatively fast kinetics compared with Shaw S4 and ILT. Notably, records in Fig. 3 show that the V369I and S376T mutants both exhibit sigmoidal activation kinetics similar to Shaker while the I372L mutant appears to activate with much less sigmoidicity (see below).

Since none of the single point mutants activate like ILT, we next tried to determine if any pairwise combination of the three substitutions, V369I, I372L, and S376T, was sufficient to produce ILT-like activation. Representative currents and normalized conductance–voltage curves for several patches with IL, LT, and IT mutants are also shown in Fig. 3. Values from Boltzmann fits to the conductance–voltage curves are presented in Table I. As with the single amino acid substitutions, there are considerable changes in the voltage range of activation and the slope of the conductance–voltage curve. The double mutants containing the I372L substitution activate more slowly than the V369I, S376T, and IT mutants, but not nearly as slowly as ILT, nor do they operate in the same voltage range nor with the same voltage dependence of opening (see Fig. 9). As with the single I372L point mutant, the two double mutants containing the I372L substitution appear to activate with less sigmoidicity than Shaker and the IT mutant. The conclusion from these experiments is that all three amino acid substitutions, V369I, I372L, and S376T, are necessary to make Shaker channels activate like Shaw S4 channels.

This result is particularly interesting since all three substitutions (valine to isoleucine, isoleucine to leucine, and serine to threonine) are very conservative. Two of the three substitutions (V369I and S376T) add a methyl group to the end of an amino acid side chain, making it larger and more hydrophobic. The third substitution, I372L, simply translocates a methyl group by one carbon, changing the branchpoint of the aliphatic side chain. The I372L substitution results in little or no change in hydrophobicity or size of the residue, though it does result in a change in shape of the side chain. The profound effects of the substitutions in ILT on

channel opening suggest that steric interactions of hydrophobic and polar side chains in the COOH-terminal portion of the S4 play an important role in the cooperative transition in the activation pathway. The large functional effects due to small physical and chemical changes introduced by these three substitutions suggest that residues in the COOH-terminal portion of each S4 are in a closely packed region of the channel protein.

These interactions do not seem to be as important in the gating of the S4 donor channel Shaw. The converse triple mutant VIS/Shaw (see Fig. 1; isoleucine to valine, leucine to isoleucine, threonine to serine in Shaw) does not appreciably alter the rate, time course, or voltage dependence of Shaw activation (data not shown). Perhaps the VIS substitutions in Shaw are better tolerated because the packing of amino acid side chains in the vicinity of the S4 is less constrained in Shaw. Alternatively, these substitutions may affect analogous transitions in the Shaw channel, but their effects are not evident due to other transitions dominating Shaw activation.

Within the K_v1 subfamily of Shaker homologs, the S4 is highly conserved across many species (Chandy and Gutman, 1995). The wild-type amino acids at the ILT positions (V369, I372, and S376) in Shaker are conserved among both Shaker and Shal homologs. Among rat Shaw homologs, the S4 is also highly conserved, as are the amino acids I369, I372, and T376 at the equivalent Shaker positions. In contrast, the S4 of *Drosophila* Shaw differs from its rat Shaw homologs in 11 of 21 amino acids. While the amino acids I369 and T376 in *Drosophila* Shaw are the same as in the rat Shaw homologs, the residue at the Shaker equivalent position 372 in *Drosophila* Shaw is a leucine rather than the isoleucine present in the rat homologs. The leucine in Shaw at this position replaces a highly conserved isoleucine that is present in most other channels. The fact that residues at these three positions, and in particular I372, are highly conserved within and across subfamilies is consistent with the large functional consequences to mutations at these sites in Shaker.

Comparison of ILT and Shaw S4 Activation

While macroscopic ionic currents from ILT are very similar to currents from Shaw S4, there are differences between them (Fig. 4). ILT channels open and close a little faster than Shaw S4 channels (Fig. 4 *B*). However, the voltage dependence of the kinetics and steady state activation are very similar. The equivalent charge associated with channel opening and closing was estimated assuming that the opening and closing kinetics of ILT and Shaw S4 are dominated by a single rate-limiting transition (see legend, Fig. 4). This assumption is reasonable since the opening and closing kinetics of both Shaw S4 and ILT are well fit by single exponential func-
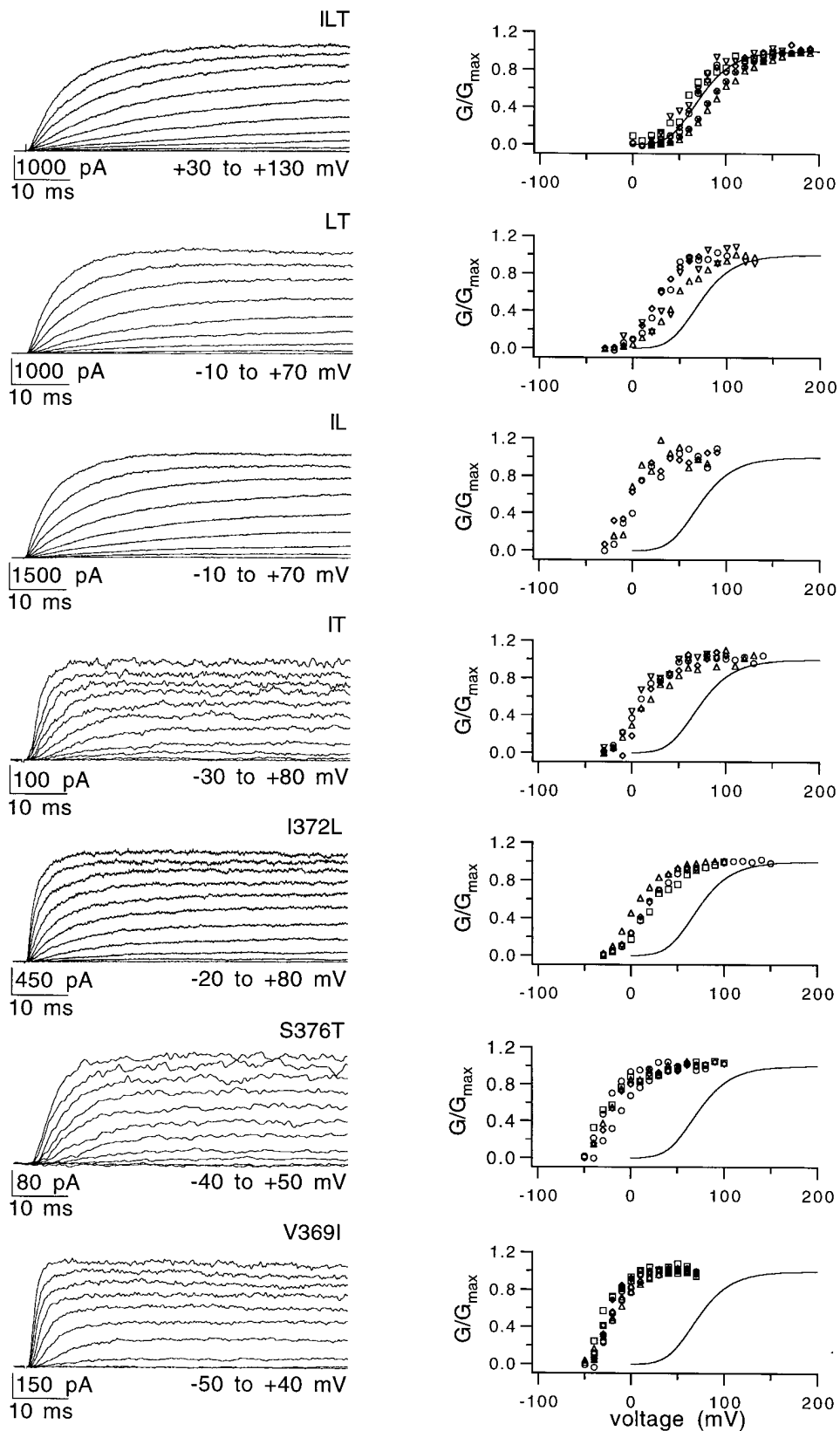
FIGURE 3. Macroscopic currents and conductance–voltage curves for single and double point mutants of ILT. On the left are representative current traces at a series of voltages, incremented by 10 mV in the voltage ranges indicated. On the right are normalized conductance–voltage curves summarizing data from several experiments, each symbol representing data from a separate patch. The solid line is a fourth power Boltzmann function representing a fit to the data for ILT, created from the mean values in Table I to ease comparison between the mutants and ILT. ILT currents were digitized at 5 kHz and filtered at 2 kHz. All other currents were digitized at 20 kHz and filtered at 8 kHz. The number of patches used for each mutant is as follows: nine for V369I, four for I372L, five for S376T, four for IT, three for IL, four for LT, and six for ILT.

tions over a wide range of voltages. The equivalent charge associated with channel opening is 0.78 and 0.85 electronic charge for Shaw S4 and ILT, respectively. These values are similar to each other and are significantly larger than the value of 0.42 electronic charge calculated for opening transitions late in the activation pathway of Shaker (Zagotta et al., 1994b). Values for equivalent charge associated with the closing transitions are estimated to be 0.86 and 0.90 electronic charge for Shaw S4 and ILT, respectively. Again, the
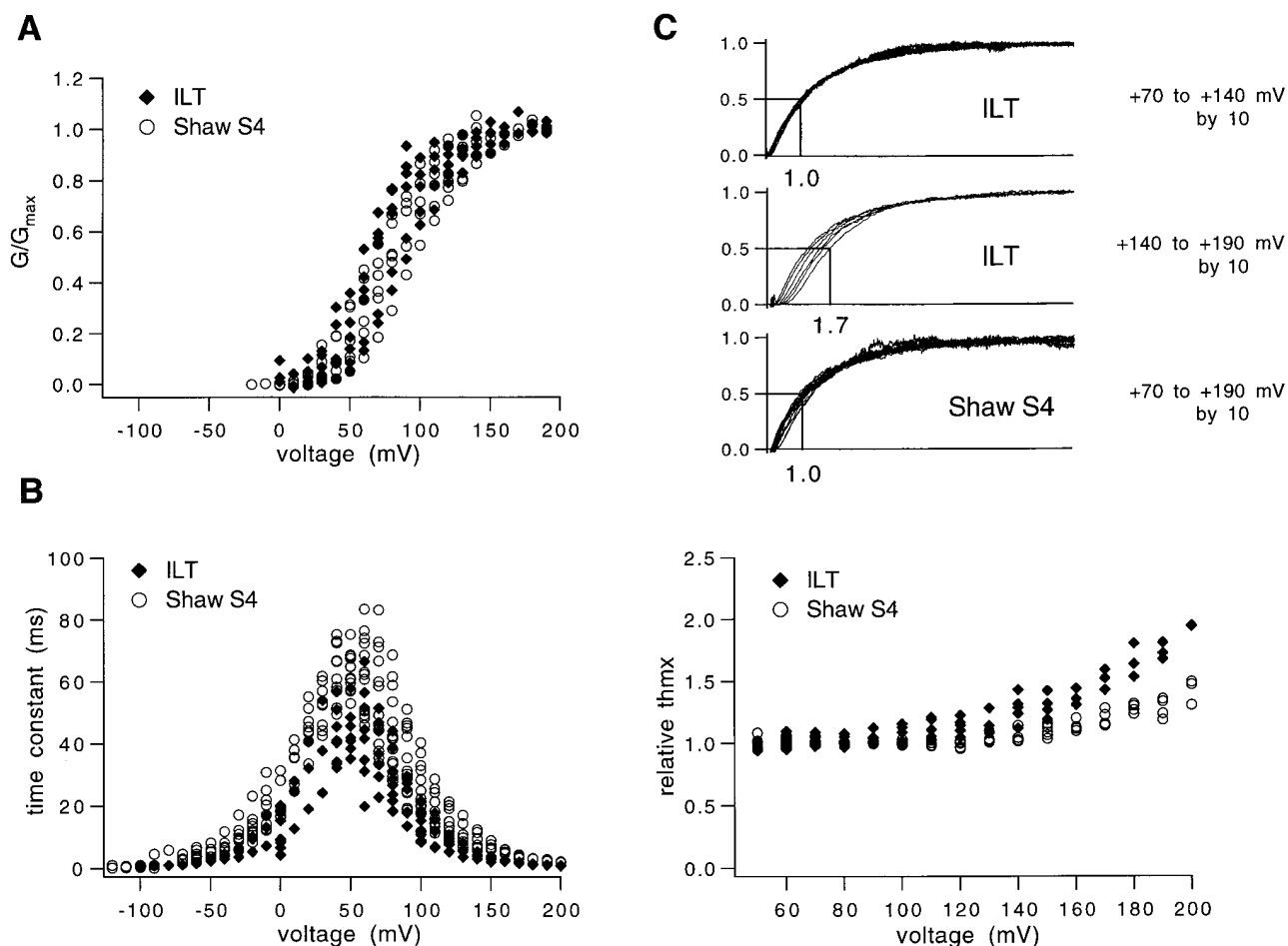

FIGURE 4. Comparison of functional properties of ILT and Shaw S4. (A) Normalized conductance plotted as a function of voltage for ILT and Shaw S4. ILT and Shaw S4 currents were digitized at 5 kHz and filtered at 2 kHz or were digitized at 20 kHz and filtered at 8 kHz. Data from six patches with ILT and six patches with Shaw S4 are compared. (B) Time constants for channel opening and closing were calculated from fits of single exponential functions to currents from ILT and Shaw S4 as outlined in MATERIALS AND METHODS. Data from 10 patches with ILT and 14 patches with Shaw S4 are shown. Estimates of equivalent charge for channel opening and closing kinetics were calculated by fitting the time constants with the following: $\tau(V) = 1/(\alpha + \beta)$, $\alpha(V) = \alpha_0 e^{(z_\alpha FV/RT)}$, $\beta(V) = \beta_0 e^{(-z_\beta FV/RT)}$. $\tau(V)$ is the time constant from single exponential fits of currents during activation and deactivation at several voltages, V. $\alpha(V)$ and $\beta(V)$ are the forward and backward rate constants at each voltage, respectively. α_0 and β_0 are the forward and backward rate constants at 0 mV, respectively. z_α and z_β are the values of the equivalent charge for opening and closing the channels, respectively. Equivalent charge estimates for the forward rates for Shaw S4 and ILT are 0.78 and 0.84 electronic charges, respectively. Equivalent charge estimates for the backward rates for Shaw S4 and ILT are 0.86 and 0.90 electronic charges, respectively. ILT currents were digitized at 20 kHz and filtered at 8 kHz. Shaw S4 currents were digitized at 5 kHz and filtered at 2 kHz or were digitized at 20 kHz and filtered at 8 kHz. (C, top). Currents for ILT and Shaw S4 scaled for comparison of sigmoidicity. Currents were scaled as outlined in MATERIALS AND METHODS to compare the relative delay in the activation time course. All values along the time axis are normalized so that when there is no delay, the relative time to half maximum current, thmx, is equal to one. Values greater than one indicate an increase in sigmoidicity. Scaled currents for Shaw S4 superimpose over a wide range of voltages, with a relative thmx of ~1, indicating little tendency toward sigmoidicity. Scaled currents for ILT are separated into two groups to show that at voltages below +140 mV, the scaled currents superimpose with a relative thmx of ~1. However, above +140 mV, there is an incremental increase in the delay with more positive voltage steps. (bottom) The relative thmx is plotted as a function of voltage, summarizing analysis of sigmoidicity from six patches with ILT channels and six patches with Shaw S4 channels. Currents from ILT and Shaw S4 were digitized at 20 kHz and filtered at 8 kHz. Little distortion in the waveform is expected or observed from delays introduced by the filter at these frequencies, due to the relatively slow rate of channel kinetics.

values for ILT and Shaw S4 are similar, though they are slightly less than the 1.1 electronic charges calculated for Shaker channel closing (Zagotta et al., 1994*b*).

Like Shaw S4, ILT activation is well fit by a single exponential function over a wide range of voltages. However, unlike Shaw S4, ILT activation deviates from single exponential kinetics at very positive voltages. We compared deviations from single exponential behavior in the two channel species by measuring the delay in activation relative to the rate-limiting transitions in the activation pathway. The scaling procedure outlined in MATERIALS AND METHODS allows us to compare the delay in activation at different voltages and between different channel species, under conditions where the current magnitude and the rates of activation vary (see also Smith-Maxwell et al., 1998; Zagotta et al., 1994*a*, 1994*b*). A channel opening with no delay and after a single exponential time course will have a relative time to half maximum current, thmx, equal to one. A value greater than one indicates the presence of delay in channel opening due to multiple voltage-dependent transitions between closed states in the activation pathway, none of which is rate limiting. For Shaw S4 and ILT, the scaled currents superimpose at voltages between +30 and +140 mV and the relative thmx of the scaled currents is approximately one (Fig. 4 *C*), suggesting that a single voltage-dependent transition is rate limiting over this entire voltage range. Above +140 mV, there is a small but progressive increase in the relative delay in the activation time course of ILT that is not nearly as pronounced in Shaw S4. This increase in relative delay at more positive voltages indicates that ILT activation includes multiple voltage-dependent transitions between closed states before the cooperative step that is rate limiting at more negative voltages. The transitions between closed states emerge at more positive voltages because the voltage dependence of the rate-limiting transition is steeper than that of many or all of the transitions between closed states.

The different voltage-dependent patterns of sigmoidicity observed for ILT and Shaw S4 could have one of several possible explanations. The rate-limiting transition of the Shaw S4 channel is a little slower than in ILT and, therefore, more positive voltage steps may be required to make the transition sufficiently fast to unmask delay due to closed-state transitions. Another possible explanation is that Shaw S4 activation involves fewer or faster closed-state transitions or perhaps involves just a single transition between one closed state and the open state. In contrast, the voltage-dependent pattern of delay in activation is much different for Shaker. At low depolarizations there is little delay, while at more depolarized voltages the amount of delay increases progressively, and then saturates (see Fig. 8; Zagotta et al. 1994*a*, 1994*b*). This pattern of delay in

Shaker can be explained by the large number of transitions between closed states with similar voltage dependences and by the nonindependent nature of the first closing transition between the open state and the last closed state (Zagotta et al., 1994*a*, 1994*b*).

A Kinetic Model for ILT

To understand further the changes in the ionic currents introduced by the substitutions in ILT, we modified an existing multi-state model developed for Shaker (Zagotta et al., 1994*a*). The rationale for this is as follows. First, the multi-state model is quite successful at accounting for the kinetic and steady state properties of wild-type Shaker activation gating at the level of gating currents, macroscopic ionic currents, and single channel currents (Zagotta et al., 1994*a*). Second, since the ILT mutant channel was constructed from three very conservative amino acid substitutions, it seems reasonable to assume that the mutant channel would activate in fundamentally the same way as Shaker, but with changes in one or more of the existing transitions. Third, the delay in ILT activation kinetics observed above +140 mV reveals the existence of other transitions in the activation pathway besides the rate-limiting transition.

The 15-state model for Shaker activation, shown in Fig. 5, is an extended representation of a kinetic scheme wherein each subunit of a channel tetramer must undergo two sequential transitions before the channel can open (Zagotta et al., 1994*a*). All horizontal transitions in the 15-state model represent the first independent and identical transition undergone by each of the four channel subunits. All vertical transitions represent subsequent identical transitions in each subunit, with the exception that the transition between the last closed state and the open state has special properties. The first closing transition is slower than expected for a purely independent process and is formally equivalent to cooperative stabilization of the open state.

We were able to account successfully for the functional properties of ILT ionic currents by changing the rates and voltage dependences of a single set of transitions between the last closed state and the open state. We focused on this set of transitions for several reasons. First, the single exponential time course of ILT channel opening implies that a single transition is rate limiting. Since the single exponential time course of activation is the result of identical mutations in each of four channel subunits, a single cooperative or concerted transition must be altered by the mutations (Smith-Maxwell et al., 1998). If instead, the mutations slow the forward rate of either set of independent transitions in the 15-state model for Shaker, the activation time course would be sigmoid and not single exponential. Second, ILT

$$C \underset{\beta}{\overset{4\alpha}{\rightleftharpoons}} C \underset{2\beta}{\overset{3\alpha}{\rightleftharpoons}} C \underset{3\beta}{\overset{2\alpha}{\rightleftharpoons}} C \underset{4\beta}{\overset{\alpha}{\rightleftharpoons}} C$$

$$\delta \updownarrow \gamma \qquad \delta \updownarrow 2\gamma \qquad \delta \updownarrow 3\gamma \qquad \delta \updownarrow 4\gamma$$

$$C \underset{\beta}{\overset{3\alpha}{\rightleftharpoons}} C \underset{2\beta}{\overset{2\alpha}{\rightleftharpoons}} C \underset{3\beta}{\overset{\alpha}{\rightleftharpoons}} C$$

$$2\delta \updownarrow \gamma \qquad 2\delta \updownarrow 2\gamma \qquad 2\delta \updownarrow 3\gamma$$

$$C \underset{\beta}{\overset{2\alpha}{\rightleftharpoons}} C \underset{2\beta}{\overset{\alpha}{\rightleftharpoons}} C$$

$$3\delta \updownarrow \gamma \qquad 3\delta \updownarrow 2\gamma$$

$$C \underset{\beta}{\overset{\alpha}{\rightleftharpoons}} C$$

$$k_c \updownarrow k_o$$

$$O$$

$$C \underset{k_c}{\overset{k_o}{\rightleftharpoons}} O$$

········ 15 state model
——— 2 state model

|————| 0 to +200 mV by 20
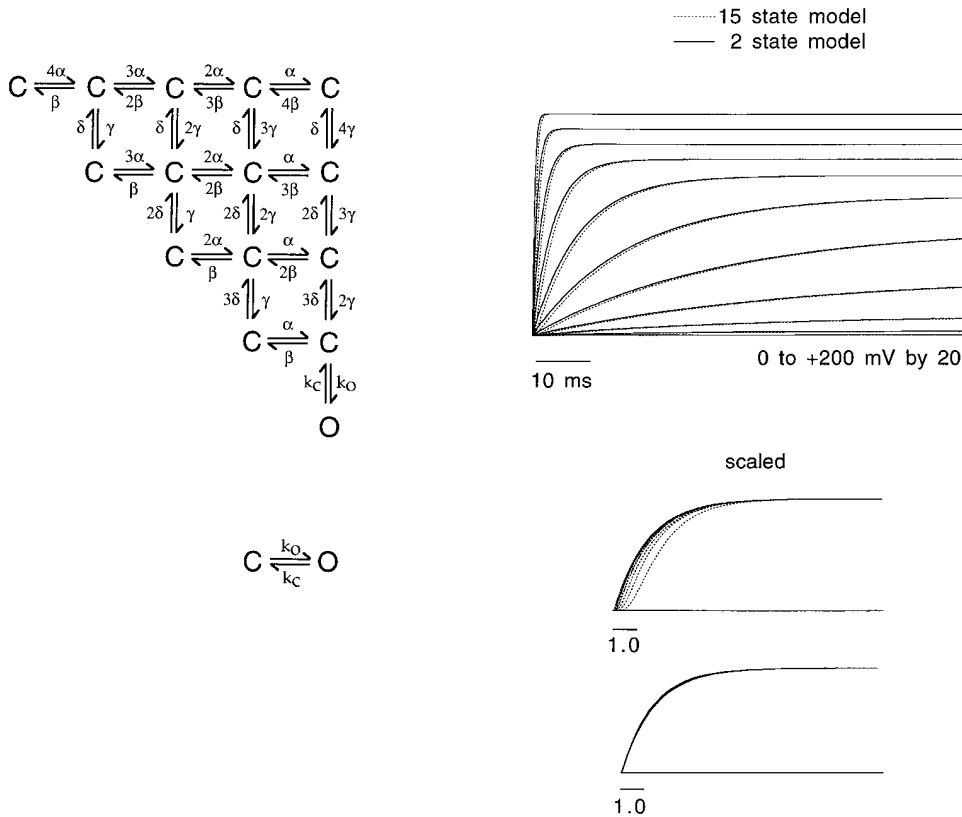10 ms

scaled

|—
1.0

|—
1.0

FIGURE 5. Kinetic models for ILT. (*left*) Schematic representations of two kinetic models designed to describe the functional behavior of ILT are shown. The parameters used to generate the 15-state model for ILT are based on a model described for Shaker potassium channels (see Fig. 7 and Table I in Zagotta et al., 1994*a*). The 0-mV rate constants and the associated equivalent charge for the final step in activation of both Shaker and ILT are given in Table II. For the simplified two-state model, the rates used to describe the opening and closing transitions, k_o and k_c, are identical to those used for the final step between the last closed state and the open state in the 15-state model for ILT. (*right*) Current simulations for ILT from the 15- and 2-state models are superimposed for direct comparison. Currents were simulated at the voltages indicated, from a holding potential of −80 mV. The traces on the bottom result from scaling the simulated currents for each of the two models for ILT as described in MATERIALS AND METHODS to highlight the difference in sigmoidal behavior predicted by the two models.

channels are much slower to open and close than Shaker channels. If the last transition in ILT activation is sufficiently slower than the preceding transitions, the slow transition would dominate the overall time course and make a multi-step activation process, like the 15-state Shaker model, appear to be a single exponential process.

Third, slowing the forward rates in either set of independent transitions will not produce the large decrease in slope observed for ILT. We showed in our previous paper (Smith-Maxwell et al., 1998) that slowing the forward rate of a set of independent transitions in a six-state model shifts the conductance–voltage relation to more positive voltages but does not decrease the slope of the curve. However, in the 15-state model for Shaker, there are two sets of independent transitions that have different voltage dependences. While slowing the rate of the forward transitions for either set of independent transitions shifts the conductance–voltage relation to more positive voltages, the slope of the curve is differentially affected. Slowing all forward rates of the first set of independent transitions has no effect on the slope of the conductance–voltage relation because these transitions dominate opening in the 15-state

Shaker model over a wide range of voltages. Slowing all forward rates in the second set of independent transitions decreases the slope because this second set of transitions now dominate activation and they move a little less charge than the first set of transitions. However, this decrease in slope is very modest compared with the dramatic decrease predicted by slowing a single forward transition or compared with the large decrease in slope observed with ILT. Therefore, altering either set of independent transitions in the 15-state model cannot explain our results.

Values for the rate constants and charge associated with the last set of transitions in the activation pathway for the Shaker and ILT models are given in Table II. Values for the earlier transitions in the multi-state ILT model are identical to those used for Shaker (see Fig. 7 and Table I in Zagotta et al., 1994*a*). To approximate the ILT ionic currents, the rate constant for the final opening transition, $k_o(0)$, is made much smaller than for Shaker, while the rate constant for the first closing transition, $k_c(0)$, is larger than for Shaker. The net effect of these modifications is to shift the probability of channel opening to more positive voltages and to slow

TABLE II

Rate Constants for Final Step In Models For Shaker, ILT, and I372L

	k_o		k_c		
	$k_o(0)$	z_o	$k_c(0)$	z_c	θ
	s^{-1}	e^- charge	s^{-1}	e^- charge	
Shaker	2800	0.32	9	1.10	9.4
ILT	1	1.00	70	0.80	1.2
I372L	27	1.00	48	0.80	1.8

Rate constants are given for transitions between the last closed state and the open state in the multistate models for Shaker, ILT, and I372L. The values for ILT are also used in the two state model for ILT (see Fig. 5). Voltage-dependent rate constants for the opening and closing transitions are given by k_o and k_c, respectively. The model assumes that the rate constants are exponentially dependent on voltage. The rate constants are described by the following expressions: $k_o = k_o(0)\,e^{z_oFV/RT}$ and $k_c = k_c(0)\,e^{-z_cFV/RT}$. $k_o(0)$ and $k_c(0)$ are the 0-mV rate constants for the opening and closing transitions, respectively, while z_o and z_c are the equivalent electronic charges for the opening and closing transitions, respectively. V is the voltage. Assuming $k_c = 4\delta/\theta$, as in the Shaker model from Zagotta et al. (see Table I, Fig. 7 in 1994*a*), θ can be calculated for each model described here.

activation kinetics substantially. The charge associated with the final opening transition in ILT is 1 electronic charge, three times larger than the 0.32 electronic charge associated with the same transition in Shaker. The charge associated with the first closing transition in ILT of 0.80 electronic charge is slightly smaller than the 1.10 electronic charges used for the same transition in Shaker. The charge incorporated into these transitions in the ILT model is comparable to the equivalent charge calculated independently in the previous section from the voltage dependence of the time constants of activation and deactivation of ILT, where 0.85 electronic charge is associated with channel opening and 0.90 electronic charge with channel closing.

The modified Shaker model successfully reproduces the voltage range and kinetics of activation and the slope of the conductance–voltage curve observed for the ILT mutant (Figs. 5 and 6). Although the predictions more closely follow the more negative conductance–voltage results, this discrepancy represents only a small energetic difference (0.4 kcal mol^{-1}, calculated from $\Delta\Delta G = z\Delta V_{1/2}$, where z is the amount of charge moved for the final transition and $\Delta V_{1/2}$ is the difference in the half activation voltage between the model and the ILT data). The time constants from single exponential fits to the simulated ionic currents are also very similar to those from fits of currents from the mutant ILT channel, as is the voltage-dependent pattern of sigmoidicity (Fig. 6).

Since ILT opening and closing kinetics are well fit by a single exponential function at voltages between −90 and +140 mV, we also simulated currents using a simple two state scheme as in Fig. 5. Values for the rate
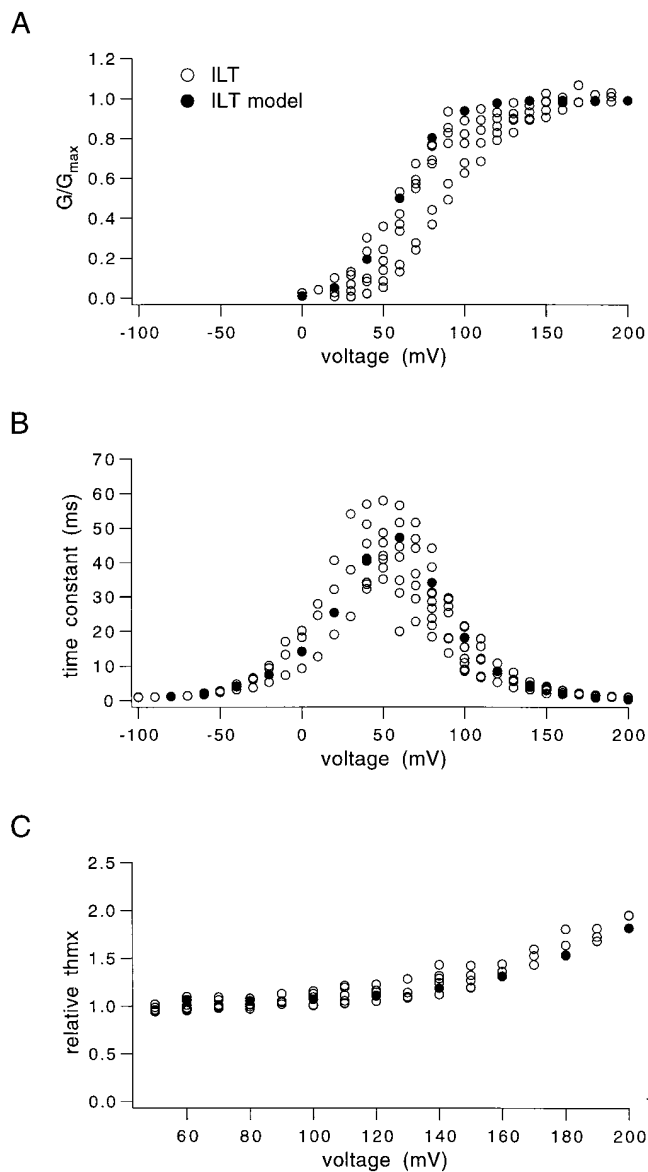

FIGURE 6. Comparison of 15-state ILT model predictions with ILT mutant data. (*A*) Voltage protocols similar to those used for the ILT mutant channels were used to simulate currents for analysis. Isochronal values of currents simulated by the model were measured at 0 mV after 300-ms positive voltage steps to activate the channel. The values from the simulated currents are normalized to the maximum value and plotted with data from the ILT mutant, replotted from Fig. 4 *A*. (*B*) Time constants were determined from the simulated currents with single exponential fits to activation and deactivation kinetics as outlined in MATERIALS AND METHODS. Time constants for the simulations are plotted as a function of voltage along with results from the ILT mutant, which are replotted from Fig. 4 *B*. (*C*) Simulated currents were scaled for analysis of sigmoidicity as outlined in MATERIALS AND METHODS. The relative time to half maximum current, thmx, is plotted with the results of analysis of the ILT mutant, replotted from Fig. 4 *C*.

constants and associated charge are the same as those used for the final transition in the multi-state model for ILT given in Table II. The simulated currents from the two-state model are very similar to simulated currents from the multi-state ILT model. The steady state probability of channel opening is the same for the two models and there is little difference in the time course of activation. The two models differ only in their prediction for whether or not there is a small delay in activation at higher voltages. When the currents are scaled to measure the relative delay in activation, there is no delay in the two-state model. The relative accuracy with which the two state model approximates the steady state properties and gating kinetics of the larger ILT model illustrates the dominance of the final rate-limiting step.

The multi-state model successfully predicts the delay in activation observed at voltages above +140 mV, seen for the ILT mutant (Figs. 4 and 5). Delay emerges at higher voltages because the final transition into the open state is no longer rate limiting. In the model, this occurs because the equivalent charge associated with the transition into the open state, z_o, is four times greater than the charge associated with the next slowest rate constant, α. Because of the steeper voltage dependence of the k_o transition, the rates of the early and late transitions approach each other at large positive voltages, and the early transitions produce a delay in activation. As can be seen in Fig. 6 C, the relative delay and the voltage dependence of the delay from the multi-state–simulated ILT currents superimpose on results from the ILT mutant channel. These results show that even though macroscopic ionic currents from the ILT mutant can be approximated by a simple two-state model over a wide voltage range, a multi-state model is required to simulate the functional properties of ILT currents over a more extended voltage range. Thus, we are able to reproduce successfully the essential features of the macroscopic ionic currents of ILT by making a very simple modification of an existing multi-state model for Shaker channel activation.

ILT Gating Currents

Our conclusion that the activation pathway of the ILT mutant resembles that of Shaker, except for the final transition, makes certain predictions about the movement of gating charge in ILT. The gating charge should move in a voltage range more negative than the voltages required to open the channel and, at voltages where the channel opens, gating currents should be detected well before the ionic currents. As shown in Fig. 7, ON gating currents from the ILT mutant follow both of these predictions. At voltage steps to between −100 and +20 mV, large gating currents are observed with no detectable ionic currents. At more positive voltages where the channels open, between +40 and +200 mV,
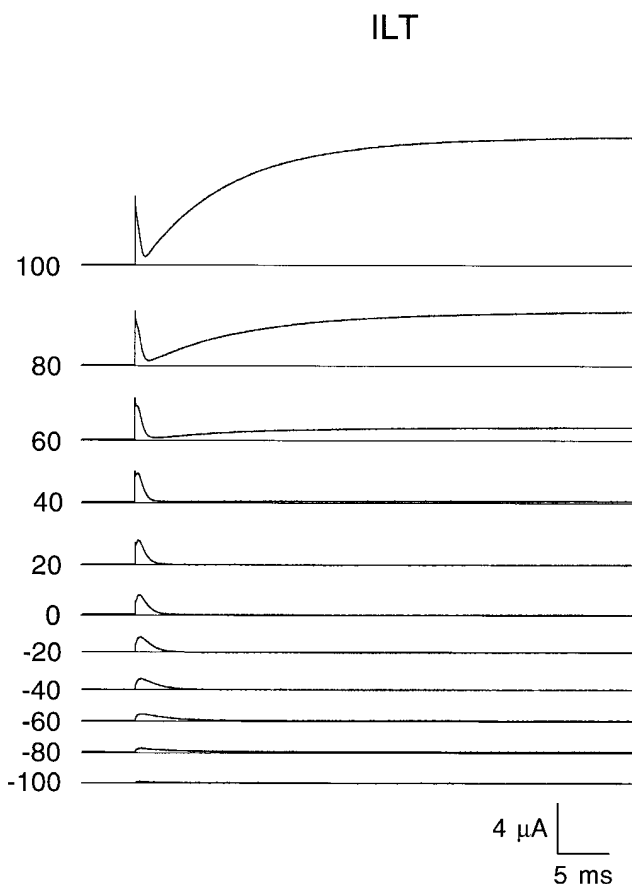
ILT

FIGURE 7.   Gating currents from conducting ILT channels. Currents were recorded at the voltages indicated (millivolts) from a holding potential of −40 mV after a 2-s prepulse to −140 mV. At voltages more positive than +30 mV, ionic currents begin to activate. Leak subtraction was done with a P/5 protocol from a leak holding potential of 0 mV. ILT gating currents were digitized at 40 kHz and filtered at 10 kHz. Currents were recorded with the cut-open oocyte voltage clamp.

the gating currents are quite rapid compared with the time course of channel opening. These results are consistent with the prediction from the altered Shaker model that activation of ILT involves multiple voltage-dependent transitions that precede a final rate-limiting step. More detailed analysis of ILT gating currents during activation and deactivation will be used to refine the model for ILT (Ledwell, J.L., and R.W. Aldrich, manuscript in preparation).

The Importance of the I372L Substitution

The I372L substitution changes the rate and voltage dependence of channel opening and the amount of sigmoidal delay in the activation time course. In fact, currents from all mutants containing the I372L substitution activate with less sigmoidal delay than mutants without the I372L substitution. The sigmoidicity of the single and double point mutants of ILT is analyzed in

Fig. 8, where the relative time to half maximum, thmx, of scaled currents is plotted as a function of voltage. All mutants with the I372L substitution are represented by filled symbols, while all other mutants are represented by open symbols. The plot shows very clearly that all mutants with the I372L substitution activate with much less sigmoidal delay than Shaker and mutants without the I372L substitution, including the mutants V369I, S376T, and IT.

Time constants from all mutants with the I372L substitution are generally slower than those without the I372L substitution and are positively shifted along the voltage axis, as are the conductance–voltage curves (Fig. 9; see also Fig. 3). The slowest time constants for mutants with the I372L substitution, between 15 and 20 ms, are still much faster than the slowest time constant for ILT, ~44 ms at +50 mV. For mutants lacking the I372L mutation, the slowest time constant is nearer 10 ms, similar to Shaker. The slower, positively shifted kinetics of the I372L-containing mutants could explain the decrease in sigmoidicity if the I372L mutation slows the final step in activation while having little effect on the relatively rapid preceding transitions. These channels would then require larger positive voltage steps to open and there would be a large discrepancy between the rate of the slower final step and the rates of the faster preceding transitions. This would make the final step rate limiting and decrease the sigmoidicity of I372L channel activation, suggesting that the I372L substitution may be the dominant mutation changing cooperativity of the final transition in all I372L-containing mutants, including ILT.

The I372L mutation also alters the voltage dependence of channel kinetics. Equivalent charge estimates for activation and deactivation kinetics from Shaw S4, Shaker, ILT, and all single and double point mutants of ILT are compared in Table III. For the I372L mutant, 0.90 electronic charges are associated with channel opening and 1.17 electronic charges are associated with channel closing. The charge associated with opening of the I372L mutant is similar to charge estimates for Shaw S4 and ILT and is more than twofold larger than the charge estimated for late transitions in the activation of Shaker (Zagotta et al., 1994*b*). The equivalent charge for closing is not significantly different from wild type. For all mutants with the I372L substitution, the charge associated with channel opening is at least twofold larger than for the other mutants and Shaker, which all contain the conserved isoleucine at position 372. This analysis suggests that the I372L mutation changes a transition in the activation pathway in each of the I372L-containing mutants, making the transition rate limiting and the voltage dependence steeper.

A Kinetic Model for I372L Activation

Activation of I372L mutant channels can be explained by modifying the rate constants and charge associated with the final transition in the multi-state model for Shaker (Fig. 5). As with the ILT model, all transitions between closed states were assigned values identical to the original Shaker model (see Fig. 7 and Table I in Zagotta et al., 1994*a*). Results from analysis of simulated currents using three different sets of parameters for the final transition are superimposed on results from analysis of I372L mutant ionic currents (Fig. 10). All three sets of parameters have the same 0-mV rate constants, but differ by the amount of charge assigned
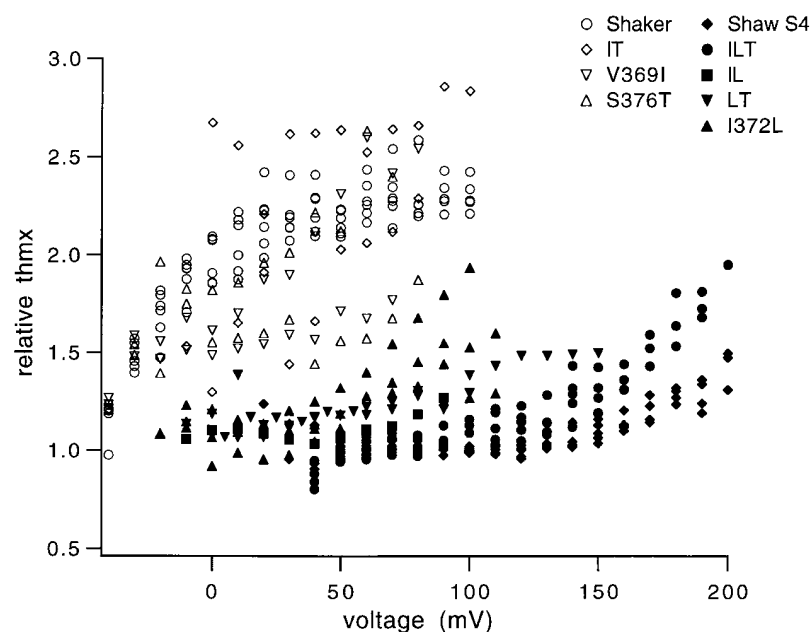

FIGURE 8. Sigmoidicity of single and double point mutants of ILT. The relative time to half maximum current (*thmx*) was plotted as a function of voltage. The number of patches for each mutant are as follows: six for Shaker, two for V369I, four for I372L, two for S376T, one for IL, four for LT, two for IT, six for ILT, and six for Shaw S4. All mutants containing the I372L substitution at position 372 are represented by filled symbols. All other channels, including Shaker, are represented by open symbols.
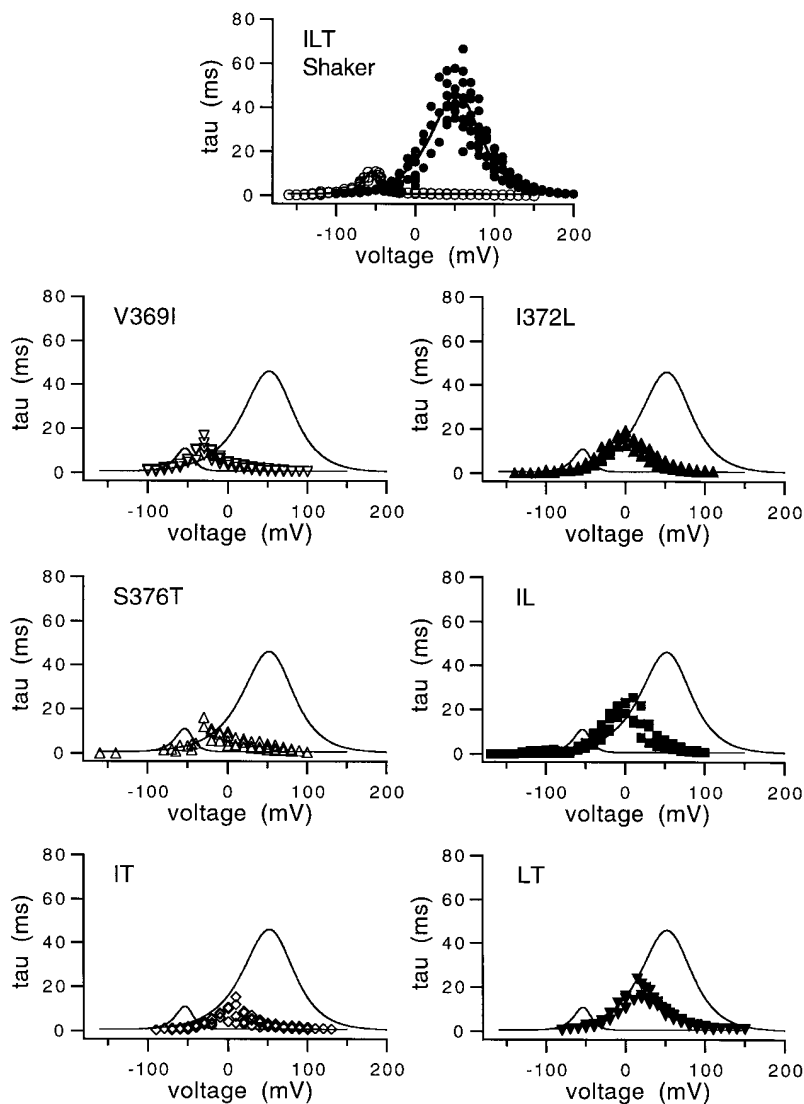
FIGURE 9. Activation kinetics for single and double ILT mutants. Time constants were calculated from fits of single exponential functions to activation and deactivation time courses, as outlined in MATERIALS AND METHODS. The number of patches for each mutant are as follows: 10 for ILT, 5 for Shaker, 5 for V369I, 4 for S376T, 4 for IT, 4 for I372L, 7 for IL, and 3 for LT. The solid lines represent fits of the time constant–voltage data for Shaker and ILT with the function $\tau = 1/(\alpha + \beta)$, where $\alpha = \alpha_0 e^{(z_\alpha FV/RT)}$ and $\beta = \beta_0 e^{(-z_\beta FV/RT)}$; τ is the time constant; α and β are the forward and backward rate constants, respectively; α_0 and β_0 are the 0 mV rate constants for the forward and backward rate constants, respectively; z_α and z_β are the charge associated with the forward and backward rate constants, respectively; and V is the voltage. For Shaker, $\alpha_0 = 2,800$ s^{-1}, $z_\alpha = 0.32$, $\beta_0 = 9$ s^{-1}, and $z_\beta = 1.1$. For ILT, $\alpha_0 = 1$ s^{-1}, $z_\alpha = 1.0$, $\beta_0 = 70$ s^{-1}, and $z_\beta = 0.8$. The lines are shown to aid comparison of the mutants with Shaker and ILT. Shaker currents were digitized at 50 kHz and filtered at 10 kHz. All other currents were digitized at 20 kHz and filtered at 8 kHz. Each mutant has the same symbol as in Fig. 8.

to the forward and backward transitions. Simulations from all three sets of parameters fit the normalized conductance–voltage curve for the I372L mutant reasonably well, but differ in how well they fit the time constants for opening and closing.

The best fits to the I372L mutant data set the equivalent charge associated with the final opening transition to the value of 1.00 electronic charge taken from the ILT model, while the worst fits use the value of 0.32 electronic charge from the Shaker model. Our analysis of I372L mutant activation kinetics estimates an equivalent charge of 0.95 electronic charge associated with channel opening, which is similar to that obtained for ILT (Table III). For the first closing transition, there is less difference between the equivalent charge used for the Shaker model of 1.1 electronic charges and for the ILT model of 0.8 electronic charge. This small difference makes it more difficult to determine whether or not the I372L substitution is responsible for the de-

crease in charge in the ILT mutant. Also, there is very little difference in how well the I372L mutant data are fit using charge values for the first closing transition from the models for Shaker or ILT.

Our analysis suggests that the I372L mutation changes the rates and voltage dependence of a cooperative transition late in the activation pathway, that we identify in our model as the transition between the last closed state and the open state. When other mutations accompany the I372L substitution, as in the ILT and Shaw S4 mutants, gating is modified further.

DISCUSSION

Substituting the S4 of Shaw into Shaker changes cooperativity in the activation pathway, decreasing the voltage dependence of channel opening and making a single cooperative transition rate limiting (Smith-Maxwell et al., 1998). In this paper, we show that simultaneous

TABLE III

	Activation	Deactivation	n
	e^- charge	e^- charge	
V369I	0.54	1.05	5
S376T	0.48	0.69	4
IT	0.43	0.83	4
Shaker	0.42	1.10	3
I372L	0.90	1.17	4
IL	1.09	1.24	7
LT	0.95	1.06	3
ILT	0.84	0.90	10
Shaw S4	0.78	0.86	14

Equivalent charge associated with activation and deactivation time constants was calculated from the time constant–voltage curves in Fig. 9. Data from all patches with a given channel species were included for each exponential fit used to calculate equivalent charge. For the I372L-containing mutants, equivalent charge was calculated by simultaneous fitting of activation and deactivation time constants, as was done for the ILT mutant in Fig. 4 *B*. As noted previously, this approach assumes that a single set of transitions is rate limiting. This assumption is reasonable for the I372L-containing mutants because there is relatively little delay in the activation time course and the kinetics are well fit by a single exponential function. The time constant–voltage curves of the I372L–containing mutants are reasonably well fit by this double exponential function. Similar values were obtained from single exponential fits to activation and deactivation time constants separately. Equivalent charge calculations for mutants without the I372L substitution come from separate fits of a single exponential to activation and deactivation time constants plotted as a function of voltage. This approach was taken since activation in these channels clearly involves multiple transitions without a single transition dominating channel opening, much like Shaker. The values for Shaker are taken from Zagotta et al. (see Figs. 7 and 11 in 1994*b*).

substitution of only three noncharged residues within the S4 of Shaker (V369I, I372L, S376T), creating the ILT mutant, is sufficient to reproduce this change in cooperativity. Ionic currents from ILT are very similar to currents from Shaw S4, while currents from the other substitution mutants that we tested are more similar to Shaker. Of particular interest is the fact that simultaneous substitution of three charged residues in the S4 of Shaker with residues from Shaw S4 (ESS) fails to reproduce the large decrease in voltage sensitivity of Shaw S4 opening. Instead, the ILT substitutions that mimic Shaw S4 activation are very conservative. While there is no change in the electrostatic charge or chemical reactivity of the residues, there are changes in hydrophobicity, size, and shape of the substituted side chains. Closely packed regions of proteins are especially sensitive to small changes in size and shape of the amino acid side chains (Eriksson et al., 1992, 1993; Creighton, 1993). Therefore, the changes in gating are likely to be mediated by differences in steric interactions. Previous work has also shown that substitution of hydrophobic residues in or near the S4 can greatly affect chan-

nel activation (Lopez et al., 1991; McCormack et al., 1991, 1993; Hurst et al., 1992; Schoppa et al., 1992; Aggarwal and MacKinnon, 1996; Tang and Papazian, 1997).

The substitution of leucine for isoleucine is responsible for the single exponential activation kinetics and the increase in the charge movement associated with the final opening transition. Yet, it is seemingly the most conservative of the three substitutions in the ILT mutant. The only structural difference between isoleucine and leucine is the point of attachment of a single methyl group along an otherwise identical aliphatic side chain. Leucine and isoleucine are both hydrophobic and have the same molecular weight and van der Waals volume. They are, however, slightly different in degree of hydrophilicity, the extent to which they tend to be found buried within proteins or on the protein surface, and the extent to which they stabilize protein secondary structures (Creighton, 1993). In spite of the small differences between the amino acids, the I372L substitution seems to be critically important for changing the properties of the final transition in the activation pathway.

The opposite substitution of isoleucine for leucine at other positions in or near the S4 has been reported previously to have large effects on steady state activation in Shaker (Hurst et al., 1992; McCormack et al., 1993). Substitution of isoleucine for leucine has been reported to have significant effects on the energetics of other proteins as well. In a study of T4 lysozyme, a leucine within the core of the protein was replaced in turn with isoleucine, valine, methionine, and phenylalanine (Eriksson et al., 1992, 1993). The isoleucine and valine substitutions decrease the stability of the folded protein by 1.4 and 2.3 kcal mol^{-1}, respectively, much more than expected from consideration of hydrophobicity and cavity formation alone. The large decrease in stability is due to steric strain introduced by replacing the leucine with a residue of a different shape. The seemingly less conservative substitutions of leucine with methionine and phenylalanine are less destabilizing than the isoleucine and valine substitutions.

Our analysis shows that the I372L substitution is responsible for the increase in equivalent charge movement associated with the final opening transition. One question that arises from this result is how substituting one uncharged amino acid for another could increase the charge movement associated with a voltage-dependent transition. The substitution could alter the movement of the voltage sensor by increasing the fraction of the electric field through which the charged residues move to open the channel or by increasing the number of charged residues that interact with the electric field. Alternatively, the final opening transition in Shaker could have the same voltage dependence as in the I372L mutant but be so fast as to be indistinguishable as a separate component in the kinetic measurements.
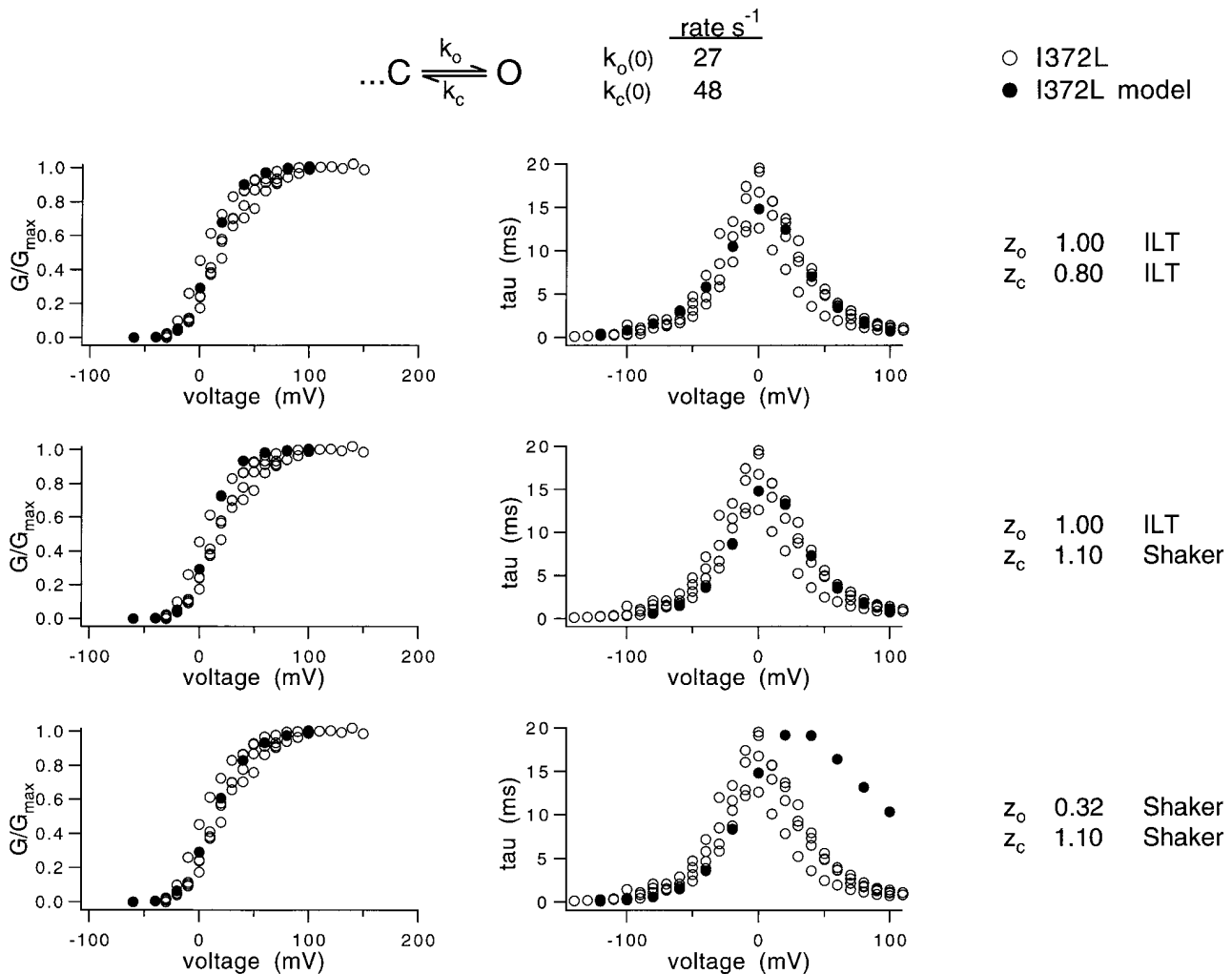
FIGURE 10. Models for I372L mutant are compared. Three different models are presented. Like the ILT model, the I372L models modify only the final step in the activation pathway of the 15-state Shaker model (see Fig. 7 and Table I in Zagotta et al., 1994a), with the values for all preceding transitions held identical to those used for Shaker. Values for the forward ($k_o(0)$) and backward ($k_c(0)$) 0-mV rate constants for the final step are given at the top of the figure and in Table II, and are the same for all three models. The models differ only by whether the charge associated with the last set of transitions is like that of Shaker or ILT. Charge associated with the forward (z_o) and backward (z_c) rate constants for each model is given (right). For Shaker, z_o equals 0.32 and z_c equals 1.1 while, for ILT, z_o equals 1.00 and z_c equals 0.80. Whether the equivalent charge used for the simulations is taken from Shaker or ILT is shown at the right. Normalized conductance–voltage curves were constructed from isochronal tail currents from the I372L mutant and from simulated currents, as outlined in MATERIALS AND METHODS. Time constants were calculated from I372L mutant currents and from currents simulated by each model, as outlined in MATERIALS AND METHODS. Data from four patches with the I372L mutant are shown. Analysis of the simulated currents is superimposed on analysis from the I372L mutant. Currents from the I372L mutant were digitized at 20 kHz and filtered at 8 kHz.

Cooperative Interactions in Activation

Subunit cooperativity seems to be a central feature in potassium channel activation. Among several kinetic models that have been proposed, there is general agreement that potassium channel activation involves transitions between multiple voltage-dependent closed states and that one or more transitions in the activation pathway involve cooperative interactions (Schoppa et al., 1992; Tytgat and Hess, 1992; Sigworth, 1993; Zagotta et al., 1994a; Bezanilla et al., 1994; McCormack et al., 1994; Hurst et al., 1995; Starkus et al., 1995). How-

ever, many details of the models differ, including the number of states, the number of independent transitions, the connectivity of the states, and the way in which the cooperativity is implemented. Cooperative interactions within proteins can come about in a number of different ways. Further analysis will be required of wild-type and mutant channels to determine the physical mechanisms underlying cooperativity in channel gating. However, simple modifications of a reasonably successful model for Shaker gating explain the effects of the ILT mutation on channel gating quite well.

Of the many transitions in the kinetic model for wild-type Shaker, it is necessary to modify only a single cooperative step to fit the ILT ionic currents, making the transition rate limiting. To model ILT, we must decrease the forward rate constant, increase the backward rate constant, increase the equivalent charge for the forward (opening) transition and decrease the charge for the backward (closing) transition. These changes are sufficient to explain the slowing of channel opening kinetics, the lack of sigmoidicity in the activation kinetics, and the changes in the voltage dependence of opening and closing kinetics compared with Shaker. These changes can also explain the large decrease in apparent voltage dependence of ILT channel opening that occurs even though there is little change in the total charge associated with channel opening. The model for wild-type Shaker channels has a total of 13.08 electronic charges, while the model for ILT has 13.46 electronic charges.

The ability of the 15-state Shaker model to explain the large differences in ILT gating with only small changes further supports the validity of the model for Shaker. A mutant such as ILT, in which a single transition is rate limiting, is useful for study of the transition in relative isolation. Since most of the transitions underlying wild-type channel activation have similar rates and voltage dependences, it is difficult to study individual transitions independently of one another (Zagotta et al., 1994a).

Results of other studies with S4 mutations in Shaker and related potassium channels can also be interpreted in terms of changes in cooperativity. Mutations at positions equivalent to 372–376 in Shaker made in eag potassium channels have been reported to cause changes in channel function similar to those observed with ILT, including a large positive shift in the voltage range of channel activation and a decrease in the slope of the conductance–voltage curve (Tang and Papazian, 1997). These results can be interpreted as a change in the cooperativity of a transition in the activation pathway and suggest that the COOH-terminal half of the S4 may serve a similar function in eag and Shaker potassium channels, mediating cooperative interactions between channel subunits. And in another Shaker homolog, $K_v1.1$, using concatenated heterotetramer constructs, Hurst et al. (1992) showed that an isoleucine substituted for a wild-type leucine present in the COOH-terminal half of the S4 alters cooperative interactions between subunits during activation.

Comparison of ILT with the hydrophobic substitution mutant, V2, located at the border between the S4 and the S4–S5 linker, provides insights into how mutations of hydrophobic residues in the S4 can alter channel activation (McCormack et al., 1991). In the V2 mutant, substitution of valine for leucine shifts the probability of channel opening to much more positive voltages and decreases the apparent voltage sensitivity of channel opening, changes similar to those observed with ILT. However, V2 and ILT have very different effects on activation kinetics. ILT activates much more slowly than Shaker and activates with a single exponential time course, whereas the time course of V2 activation is relatively rapid and sigmoid, like the time course of Shaker activation. In all, three different classes of Shaker model have been modified to explain the functional behavior of V2 (Schoppa et al., 1992; Sigworth, 1993; McCormack et al., 1994). All include several independent transitions and at least one cooperative transition late in the activation pathway. For all three models, it is necessary to alter the properties of a cooperative transition to simulate the V2 mutation. The specific details of the models may, therefore, be less important than the fact that it is necessary to change cooperativity to simulate the effect of the mutation.

Even though the apparent voltage dependence of channel opening is decreased, the total amount of charge moved to open the V2 channel is not changed. Gating currents from the V2 mutant show that while most of the gating charge moves in a voltage range similar to the wild-type channel, there is a small component of gating charge, between 18 and 19% of the total (as calculated from the model), that moves at more positive voltages (Schoppa et al., 1992). This small, positively shifted component of gating charge corresponds to the charge movement associated with the final voltage-dependent transitions. The apparent decrease in the voltage dependence of the probability of channel opening reflects the isolation of the final rate-limiting step in the activation pathway.

A similar small, positively shifted component of gating charge, comprising 13–14% of the total charge, is predicted for the ILT mutant as well. ILT gating current measurements confirm that gating charge moves in a negative voltage range where the channel does not open. Since the kinetics of the rate-limiting step in ILT activation are voltage dependent, there must be another component of gating current in the voltage range of channel opening (Ledwell et al., 1997).

Separation of charge components along the voltage axis has been observed with other S4 mutations as well. The mutant ShΔ10, studied by Aggarwal and MacKinnon (1996), substitutes the nonbasic and mostly hydrophobic residues from the S4 of $K_v2.1$ (*drk1*) into Shaker. The charge separation this generates is even greater than that found with V2. Mutations causing separation of gating charge are not confined to hydrophobic substitution mutations but also have been observed with neutralization of positive charges in the S4, including glutamine substitutions of the second and third basic residues (Perozo et al., 1994; Aggarwal and MacKin-

non, 1996; Seoh et al., 1996). However, substitution of the third basic residue with asparagine does not cause separation of gating charge components.

Channel Structure and Conformational Changes

The folded structure of proteins is maintained by multiple interactions, including hydrogen bonds, van der Waals interactions, and hydrophobic interactions (Creighton, 1993). Since the S4 has a mix of hydrophobic, polar, and basic residues, many different types of interactions may contribute to stabilizing the S4 segment within different conformational states of the channel protein. Several lines of evidence suggest that upon activation many residues in the S4 experience a change in their relative exposure to hydrophobic and aqueous environments and, therefore, may encounter different types of interactions along the activation pathway (McCormack et al., 1993; Starkus et al., 1995; Yang and Horn 1995; Yang et al., 1996; Larsson et al., 1996; Mannuzzu et al., 1996; Yusaf et al., 1996).

While the secondary structure of the S4 segment is not yet known, there is evidence that the secondary structure of the COOH-terminal half of the S4 is important in channel activation. In the rat Shaker homolog, $K_v1.1$, substitution of hydrophobic residues at two different sites within the COOH-terminal half of the S4 with proline, an amino acid known to destabilize both alpha helices and beta sheets (Richardson and Richardson, 1989), alters the ability of channels to activate (Hurst et al., 1995). These results support findings by McCormack et al. (1993) from hydrophobic substitutions in the S4–S5 that secondary structure in this region, which includes the overlapping structural motifs of periodic charged residues throughout the S4 and a leucine heptad repeat in the COOH-terminal portion of the S4, plays an important role in channel activation. The valine to isoleucine and isoleucine to leucine substitutions, as found in the ILT mutant, promote stabilization of alpha helical conformations, whereas the serine to threonine substitution does not (Creighton, 1993). If the COOH-terminal half of the S4 is alpha helical, all three substitutions would lie on the same face of the alpha helix, along a 10–11 Å stretch of the helical axis. The three residues could comprise a surface that interacts with other regions of the channel. If the S4 is alpha helical and the charged residues of the S4 interact with the charged residues of the S2 and S3, as has been suggested (Papazian et al., 1995; Seoh et al., 1996; Planells-Cases et al., 1995; Tiwari-Woodruff et al., 1997), the helical face of the S4 with the ILT substitutions would be directed away from the S2 and S3 segments.

REFERENCES

Aggarwal, S., and R. MacKinnon. 1996. Contribution of the S4 segment to gating charge in the *Shaker* K$^+$ channel. *Neuron.* 16:1169–1177.

Almers, W. 1978. Gating currents and charge movements in excitable membranes. *Rev. Physiol. Biochem. Pharmacol.* 82:96–190.

Bezanilla, F., E. Perozo, and E. Stefani. 1994. Gating of *Shaker* K$^+$ channels: II. The components of gating currents and a model of channel activation. *Biophys. J.* 66:1011–1021.

Butler, A., A. Wei, K. Baker, and L. Salkoff. 1989. A family of putative potassium channel genes in *Drosophila. Science.* 243:943–947.

Chandy, K.G., and G.A. Gutman. 1995. Voltage-gated K$^+$ channels. *In* Handbook of Receptors and Channels. Ligand- and Voltage-Gated Ion Channels. R.A. North, editor. CRC Press, Boca Raton, FL. 1–71.

Creighton, T.E. 1993. Proteins. Structures and Molecular Properties. 2nd ed. W.H. Freeman and Co., New York. 507 pp.

Eriksson, A.E., W.A. Baase, and B.W. Mathews. 1993. Similar hydrophobic replacements of Leu99 and Phe153 within the core of T4 lysozyme have different structural and thermodynamic consequences. *J. Mol. Biol.* 229:747–769.

Eriksson, A.E., W.A. Baase, X.J. Zhang, D.W. Heinz, M. Blaber, E.P. Baldwin, and B.W. Matthews. 1992. Response of a protein structure to cavity-creating mutations and its relation to the hydrophobic effect. *Science.* 255:178–183.

Hamill, O.P., A. Marty, B. Neher, B. Sakmann, and F.J. Sigworth. 1981. Improved patch clamp techniques for high-resolution current recording from cells and cell-free membrane patches. *Pflügers Archiv.* 391:85–100.

Hurst, R.S., M.P. Kavanaugh, J. Yakel, J.P. Adelman, and R.A. North. 1992. Cooperative interactions among subunits of a voltage-dependent potassium channel. *J. Biol. Chem.* 267:23742–23745.

Hurst, R.S., R.A. North, and J.P. Adelman. 1995. Potassium channel assembly from concatenated subunits: effects of proline substitutions in S4 segments. *Receptors Channels.* 3:263–272.

Larsson, H.P., O.S. Baker, D.S. Dhillon, and E.Y. Isacoff. 1996. Transmembrane movement of the *Shaker* K$^+$ channel S4. *Neuron.* 16:387–397.

Ledwell, J.L., C. Smith-Maxwell, and R.W. Aldrich. 1997. Conservative substitutions at noncharged residues in S4 that slow a coop-

erative transition in the activation pathway greatly alter voltage-dependence of gating. *Biophys. J.* 72:*A*341. (Abstr.)

Liman, E.R., P. Hess, F. Weaver, and G. Koren. 1991. Voltage-sensing residues in the S4 region of a mammalian K^{+} channel. *Nature.* 353:752–756.

Logothetis, D.E., B.F. Kammen, K. Lindpaintner, D. Bisbas, and B. Nadal-Ginard. 1993. Gating charge differences between two voltage-gated K^{+} channels are due to the specific charge content of their respective S4 regions. *Neuron.* 10:1121–1129.

Logothetis, D.E., S. Movahedi, C. Satler, K. Lindpaintner, and B. Nadal-Ginard. 1992. Incremental reductions of a positive charge within the S4 region of a voltage-gated K^{+} channel result in corresponding decreases in gating charge. *Neuron.* 8:531–540.

Lopez, G.A., Y.N. Jan, and L.Y. Jan. 1991. Hydrophobic substitution mutations in the S4 sequence alter voltage-dependent gating in *Shaker* K^{+} channels. *Neuron.* 7:327–336.

Mannuzzu, L.M., M.M. Moronne, and E.Y. Isacoff. 1996. Direct physical measure of conformational rearrangement underlying potassium channel gating. *Science.* 271:213–216.

McCormack, K., W.J. Joiner, and S.H. Heinemann. 1994. A characterization of the activating structural rearrangements in voltage-dependent *Shaker* K^{+} channels. *Neuron.* 12:301–315.

McCormack, K., L. Lin, and F.J. Sigworth. 1993. Substitution of a hydrophobic residue alters the conformational stability of *Shaker* K^{+} channels during gating and assembly. *Biophys. J.* 65:1740–1748.

McCormack, K., M.A. Tanouye, L.E. Iverson, J.-W. Lin, M. Ramaswami, T. McCormack, J.T. Campanelli, M.K. Mathew, and B. Rudy. 1991. A role for hydrophobic residues in the voltage-dependent gating of *Shaker* K^{+} channels. *Proc. Natl. Acad. Sci. USA.* 88:2931–2935.

Papazian, D.M., X.M. Shao, S.-A. Seoh, A.F. Mock, Y. Huang, and D.H. Wainstock. 1995. Electrostatic interactions of S4 voltage sensor in *Shaker* K^{+} channel. *Neuron.* 14:1293–1301.

Papazian, D.M., L.C. Timpe, Y.N. Jan, and L.Y. Jan. 1991. Alteration of voltage-dependence of *Shaker* potassium channel by mutations in the S4 sequence. *Nature.* 349:305–310.

Planells-Cases, R., A.V. Ferrer-Montiel, C.D. Patten, and M. Montal. 1995. Mutation of conserved negatively charged residues in the S2 and S3 transmembrane segments of a mammalian K^{+} channel selectively modulates channel gating. *Proc. Natl. Acad. Sci. USA.* 92:9422–9426.

Perozo, E., R. MacKinnon, F. Bezanilla, and E. Stefani. 1993. Gating currents from a nonconducting mutant reveal open-closed conformations in Shaker K^{+} channels. *Neuron.* 11:353–358.

Perozo, E., L. Santacruz-Toloza, E. Stefani, F. Bezanilla, and D.M. Papazian. 1994. S4 mutations alter gating currents of *Shaker* K channels. *Biophys.J.* 66:345–354.

Richardson, J.S., and D.C. Richardson. 1989. Principles and patterns of protein conformation. *In* Prediction of Protein Structure and the Principles of Protein Conformation. G.D. Fasman, editor. Plenum Publishing Corp., New York. 1–98.

Sanger, F., S. Nicklen, and A.R. Coulson. 1977. DNA sequencing with chain-terminating inhibitors. *Proc. Natl. Acad. Sci. USA.* 74: 5463–5467.

Schoppa, N.E., K. McCormack, M.A. Tanouye, and F.J. Sigworth. 1992. The size of gating charge in wild-type and mutant *Shaker* potassium channels. *Science.* 255:1712–1715.

Schwarz, T.L., B.L. Tempel, D.M. Papazian, Y.N. Jan, and L.Y. Jan. 1988. Multiple potassium-channel components are produced by alternative splicing at the *Shaker* locus in *Drosophila. Nature.* 331: 137–142.

Seoh, S.-A., D. Sigg, D.M. Papazian, and F. Bezanilla. 1996. Voltage-sensing residues in the S2 and S4 segments of the *Shaker* K^{+} channel. *Neuron.* 16:1159–1167.

Sigg, D., and F. Bezanilla. 1997. Total charge movement per channel. The relation between gating charge displacement and the voltage sensitivity of activation. *J. Gen. Physiol.* 109:27–39.

Sigworth, F.J. 1993. Voltage gating of ion channels. *Q. Rev. Biophys.* 27:1–40.

Smith-Maxwell, C.J., M. Kanevsky, and R.W. Aldrich. 1993. Potassium channel activation can be slowed by mutations in the S4 and S4-S5 linker regions. *Biophys. J.* 64:*A*200. (Abstr.)

Smith-Maxwell, C.J., J.L. Ledwell, and R.W. Aldrich. 1998. Role of the S4 in cooperativity of voltage-dependent potassium channel activation. *J. Gen. Physiol.* 111:399–420.

Smith-Maxwell, C.J., R.A. Taylor, and R.W. Aldrich. 1994. Amino acids responsible for slowing activation kinetics in *Shaker* potassium channel mutants. *Soc. Neurosci. Abstr.* 20:863. (Abstr.)

Starkus, J.G., T. Schlief, M.D. Rayner, and S.H. Heinemann. 1995. Unilateral exposure of *Shaker* B potassium channels to hyperosmolar solutions. *Biophys. J.* 69:860–872.

Taglialatela, M., L. Toro, and E. Stefani. 1992. Novel voltage clamp to record small, fast currents from ion channels expressed in *Xenopus* oocytes. *Biophys. J.* 61:78–82.

Tang, C.-Y., and D.M. Papazian. 1997. Transfer of voltage independence from a rat olfactory channel to the *Drosophila* ether-à-go-go K^{+} channel. *J. Gen. Physiol.* 109:301–311.

Tempel, B.L., D.M. Papazian, T.L. Schwarz, Y.N. Jan, and L.Y. Jan. 1987. Sequence of a probable potassium channel component encoded at *Shaker* locus of *Drosophila. Science.* 237:770–775.

Tiwari-Woodruff, S.K., C.T. Schulteis, A.F. Mock, and D.M. Papazian. 1997. Electrostatic interactions between transmembrane segments mediate folding of Shaker K^{+} channel subunits. *Biophys. J.* 72:1489–1500.

Tytgat, J., and P. Hess. 1992. Evidence for cooperative interactions in potassium channel gating. *Nature.* 359:420–423.

Yang, N., A.L. George, Jr., and R. Horn. 1996. Molecular basis of charge movement in voltage-gated sodium channels. *Neuron.* 16: 113–122.

Yang, N., and R. Horn. 1995. Evidence for voltage-dependent S4 movement in sodium channels. *Neuron.* 15:213–218.

Yusaf, S.P., D. Wray, and A. Sivaprasadarao. 1996. Measurement of the movement of the S4 segment during the activation of a voltage-gated potassium channel. *Pflügers Archiv.* 433:91–97.

Zagotta, W.N., T. Hoshi, and R.W. Aldrich. 1994*a. Shaker* potassium channel gating III: evaluation of kinetic models for activation. *J. Gen. Physiol.* 103:321–362.

Zagotta, W.N., T. Hoshi, J. Dittman, and R.W. Aldrich. 1994*b. Shaker* potassium channel gating II: transitions in the activation pathway. *J. Gen. Physiol.* 103:279–319.